J|A|C|S ARTICLES

Published on Web 08/21/2009

Transforming Carbon Nanotube Devices into Nanoribbon Devices

Zengxing Zhang, Zhengzong Sun, Jun Yao, Dmitry V. Kosynkin, and James M. Tour*

Department of Chemistry and the Smalley Institute for Nanoscale Science and Technology, Rice University, MS-222, 6100 Main Street, Houston, Texas 77005

Received June 15, 2009; E-mail: tour@rice.edu

Abstract: Reported here is an extension of the nanotube longitudinal unzipping process to convert electrode-bound multiwalled carbon nanotube (MWCNT) devices into graphene nanoribbon devices. Microscopy and Raman spectroscopy were used to monitor the conversion process. The electrical properties of the devices were characterized. The efficacy of the unzipping protocol on device-bound MWCNTs is demonstrated.

Introduction

Graphene is a new two-dimensional nanomaterial with novel accessible properties including room-temperature quantum hall effects, mass-less Dirac fermions, high charge carrier concentration, and mobility, making it an attractive material for use in electronics.[1−5] Several methods, including physical mechanical exfoliation,[2−4] chemical solution exfoliation,[6−10] and chemical vapor deposition (CVD) or epitaxial growth[5,11,12] have been developed to produce graphene nanostructured devices. Carbon nanotube (CNT) devices have enjoyed much attention over the past decade, and numerous embodiments have been fabricated from these rigid one-dimensional carbon structures.[13−15] Recently, our group found that bulk CNTs dispersed in concentrated sulfuric acid (H_2SO_4) can be longitudinally unzipped into graphene oxide nanoribbons (GONRs).[16] In this report, using this unzipping protocol on prebound CNT device structures, a direct conversion of the tube to a ribbon-based device was achieved. This complements a method recently disclosed by Dai to convert surface-bound CNTs into nanoribbons for device configurations.[17]

Experimental Section

To produce the CNT devices here, we used commercial multiwalled CNTs (MWCNTs) from Mitsui & Co., Ltd. as the source material (Endo's method, Lot No. 05072001K28). The MWCNTs were first ultrasonically dispersed into chloroform (CH_3Cl), and then the dispersion was spin-coated onto 200-nm oxide/silicon substrates. Through this method, the MWCNTs can be assembled on the substrates as individuals. We then fabricated devices by e-beam lithography atop the isolated MWCNTs using platinum (Pt) films.

The electrode-bound MWCNTs were then prepared for oxidative unzipping. In a typical protocol, concentrated H_2SO_4 (10 mL) in a bottle was placed in an oil bath at 55 °C, and then $KMnO_4$ (100 mg, 0.63 mmol) was added. After the mixture was stirred to produce a solution, the fabricated MWCNT devices were immersed in the solution. Following the 90 min reaction, the devices were removed and rinsed with deionized (DI) water and dried in a gentle nitrogen gas flow.

It has been shown that graphene oxide (GO) starts losing oxygen when heated to about 200 °C;[18] heat can therefore be used to reduce GONRs to nanoribbons (NRs). To reduce the unzipped devices, we heated the samples at 350 °C for 6 h under H_2 and Ar.

The morphologies of the devices were characterized with SEM (GEOL 6500) and AFM (Digital Instruments Nanoscope III A, in tapping mode). Raman spectra were measured with a Renishaw Raman scope equipped with a 514.5 nm Ar ion laser. The electrical properties were tested using a probe station at room temperature

(1) Geim, A. K.; Novoselov, K. S. *Nat. Mater.* **2007**, *6*, 183–191.
(2) Novoselov, K. S.; Geim, A. K.; Morozov, S. V.; Jiang, D.; Zhang, Y.; Dubonos, S. V.; Grigorieva, I. V.; Firsov, A. A. *Science* **2004**, *306*, 666–669.
(3) Novoselov, K. S.; Geim, A. K.; Morozov, S. V.; Jiang, D.; Katsnelson, M. I.; Grigorieva, I. V.; Dubonos, S. V.; Firsov, A. A. *Nature* **2005**, *438*, 197–200.
(4) Zhang, Y. B.; Tan, Y. W.; Stormer, H. L.; Kim, P. *Nature* **2005**, *438*, 201–204.
(5) Berger, C.; Song, Z. M.; Li, X. B.; Wu, X. S.; Brown, N.; Naud, C.; Mayou, D.; Li, T. B.; Hass, J.; Marchenkov, A. N.; Conrad, E. H.; First, P. N.; de Heer, W. A. *Science* **2006**, *312*, 1191–1196.
(6) Hernandez, Y.; et al. *Nat. Nanotechnol.* **2008**, *3*, 563–566.
(7) Li, X. L.; Zhang, G. Y.; Bai, X. D.; Sun, X. M.; Wang, X. R.; Wang, E.; Dai, H. J. *Nat. Nanotechnol.* **2008**, *3*, 538–542.
(8) Tung, V. C.; Allen, M. J.; Yang, Y.; Kaner, R. B. *Nat. Nanotechnol.* **2008**, *4*, 25–29.
(9) Stankovich, S.; Piner, R. D.; Nguyen, S. T.; Ruoff, R. S. *Carbon* **2006**, *44*, 3342–3347.
(10) Schniepp, H. C.; Li, J. L.; McAllister, M. J.; Sai, H.; Herrera-Alonso, M.; Adamson, D. H.; Prud'homme, R. K.; Car, R.; Saville, D. A.; Aksay, I. A. *J. Phys. Chem. B* **2006**, *110*, 8535–8539.
(11) Reina, A.; Jia, X. T.; Ho, J.; Nezich, D.; Son, H. B.; Bulovic, V.; Dresselhaus, M. S.; Kong, J. *Nano Lett.* **2009**, *9*, 30–35.
(12) Coraux, J.; N'Diaye, A. T.; Busse, C.; Michely, T. *Nano Lett.* **2008**, *8*, 565–570.
(13) Avouris, P.; Chen, Z. H.; Perebeinos, V. *Nat. Nanotechnol.* **2007**, *2*, 605–615.
(14) Dai, H. J. *Acc. Chem. Res.* **2002**, *35*, 1035–1044.
(15) Jin, Z.; Chu, H. B.; Wang, J. Y.; Hong, J. X.; Tan, W. C.; Li, Y. *Nano Lett.* **2007**, *7*, 2073–2079.
(16) Kosynkin, D. V.; Higginbotham, A. M.; Sinitskii, A.; Lomeda, J. R.; Dimiev, A.; Price, B. K.; Tour, J. M. *Nature* **2009**, *458*, 872–876.
(17) Jiao, L. Y.; Zhang, L.; Wang, X. R.; Diankov, G.; Dai, H. J. *Nature* **2009**, *458*, 877–880.
(18) Lomeda, J. R.; Doyle, C. D.; Kosynkin, D. V.; Hwang, W. F.; Tour, J. M. *J. Am. Chem. Soc.* **2008**, *130*, 16201–16206.

10.1021/ja9045923 CCC: $40.75

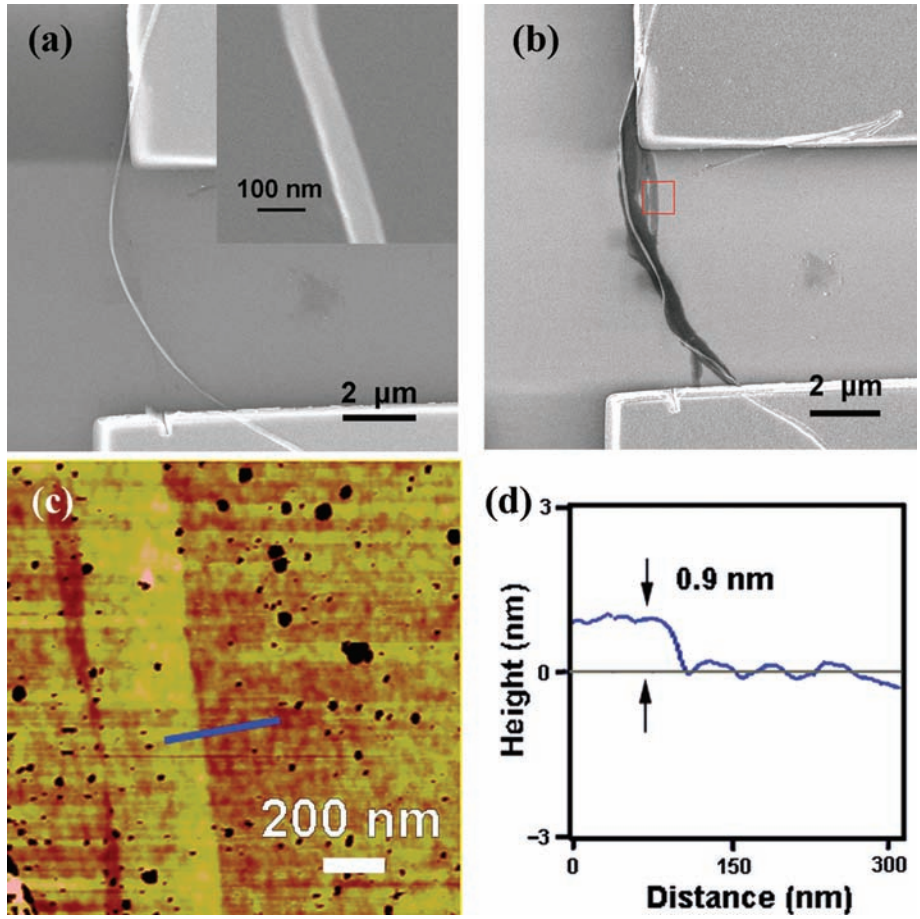

Figure 1. Morphology analysis of a typical device. (a) SEM image of a MWCNT-based device before oxidative unzipping. The inset is a magnified SEM image of the MWCNT, indicating the diameter of the MWCNT is about 70 nm. (b) SEM image of the same device after oxidative unzipping to form the nanoribbon structures. (c) AFM image of the portion of the nanoribbons in the red box in b. (d) Height profile along the line shown in c, indicating that the thickness of the nanoribbon is 0.9 nm and therefore most likely single-layered.

under vacuum (10^{-6} Torr). The electrical data were collected with an Agilent 4155C semiconductor parameter analyzer.

Results and Discussion

Figure 1a shows a SEM image of a typical MWCNT device. And Figure 1b is the SEM image of the same device as in Figure 1a after reaction with $KMnO_4$. It is obvious that treatment has changed the device. Whereas before treatment the MWCNT between the two electrodes was tens of nm in width, after the treatment it was hundreds of nm in width. At either end nearest the electrodes the MWCNTs partially or wholly retained their structure, similar to a ribbon that has had both ends closed into cylinders. The portions of the MWCNTs under the Pt electrodes were protected from unzipping, preserving the electrical contact between the electrodes and the MWCNTs. It is difficult to microscopically assess whether the smallest diameter part of the MWCNT had unzipped along the entire channel length or whether the imaged line in Figure 1b is part of a stacked-ribbon edge; however, the large excess of $KMnO_4$ and the extended time of the reaction would suggest that the smaller diameter, and hence more oxidatively reactive portion of the MWCNT, would also be converted into a nanoribbon.

As seen in Figure 1b, the unzipped MWCNT is comprised of undulating flattened structures. In the portion indicated by the red square, there are two narrow nanoribbons attached to the main nanostructure. Atomic force microscopy (AFM) in tapping mode was used to characterize the area in the box, and, as shown in Figure 1c and d, the thickness of the nanoribbon is

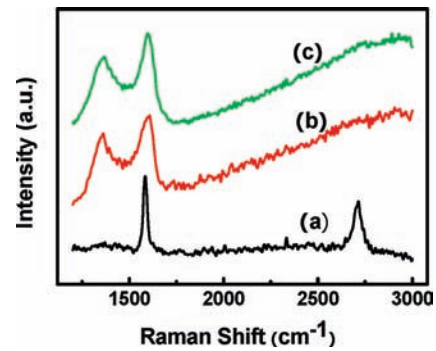

Figure 2. Raman spectra of a device at different stages. (a) MWCNT device before treatment with $KMnO_4$ with a G band at ~1585 cm^{-1} and 2D band at ~2715 cm^{-1}; (b) as-unzipped GONR device, in which the 2D band has disappeared and a new D band at ~1363 cm^{-1} has appeared; and (c) unzipped GONR device after thermal treatment, with little change in the Raman from b. Raman spectroscopy was done using a 514.5 nm Ar ion laser at room temperature.

0.9 nm. This thickness is close to the reported theoretical and experimental values for the thickness of single-layer GO,[10,19,20] and in further accordance with previous evidence from this oxidative protocol showing the formation of GONRs from MWCNTs.[16]

(19) Gomez-Navarro, C.; Weitz, R. T.; Bittner, A. M.; Scolari, M.; Mews, A.; Burghard, M.; Kern, K. *Nano Lett.* **2007**, *7*, 3499–3503.
(20) Luo, Z. T.; Lu, Y.; Somers, L. A.; Charlie Johnson, A. T. *J. Am. Chem. Soc.* **2009**, *131*, 898–899.

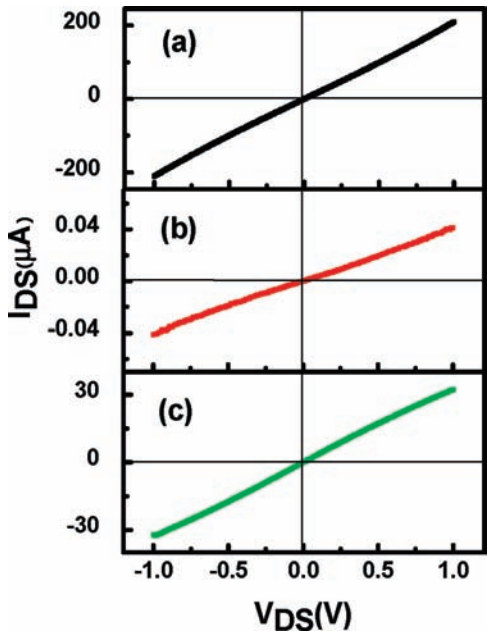

Figure 3. Electrical characteristics of the device from Figure 1 at different stages. (a) As-prepared MWCNT device. (b) After treatment with $KMnO_4$ to produce the NRs device. (c) GONR in the device after thermal treatment.

Raman spectroscopy is a powerful tool to study carbon materials. Here we used Raman spectroscopy to monitor the conversion process. Figure 2 shows a series of Raman spectra recorded from the same device. Clearly, the 2D (~2715 cm^{-1}) band in the spectrum of the single MWCNT-based device disappears after unzipping and a large D band appears at ~1363 cm^{-1}. This phenomenon is the inverse of the process that graphitizes MWCNTs,[21] indicating that the structure of MWCNT is destroyed in the oxidative unzipping process. The Raman spectrum of the unzipped device is similar to the Raman spectra reported for GO.[18,22] The Raman spectra are further confirmation that the MWCNT between the electrodes is converted into GONRs.

The Raman spectrum of the thermally reduced graphene nanoribbon device is different from mechanically exfoliated graphene.[23] The high D band in the spectrum indicates that the carbon material is still compromised of significant carbon-sp^3-hybridized sites. Comparing the Raman spectrum of the as-unzipped nanoribbon device (Figure 2b) and the thermally reduced nanoribbon device (Figure 2c), there is no obvious difference, similar to the results reported by others.[24] This can be attributed to remaining hydroxyl groups along the graphene plane and the fact that the edges are a significant portion of the NR structure relative to the small amount of edges in large-area nonribbon graphene. Nevertheless, the thermal reduction of the devices leads to a significant improvement in the conductivity of the devices.

Figure 3 shows the $I_{DS}-V_{DS}$ curves of a typical device at different stages. As shown in Figure 1, the sections of the

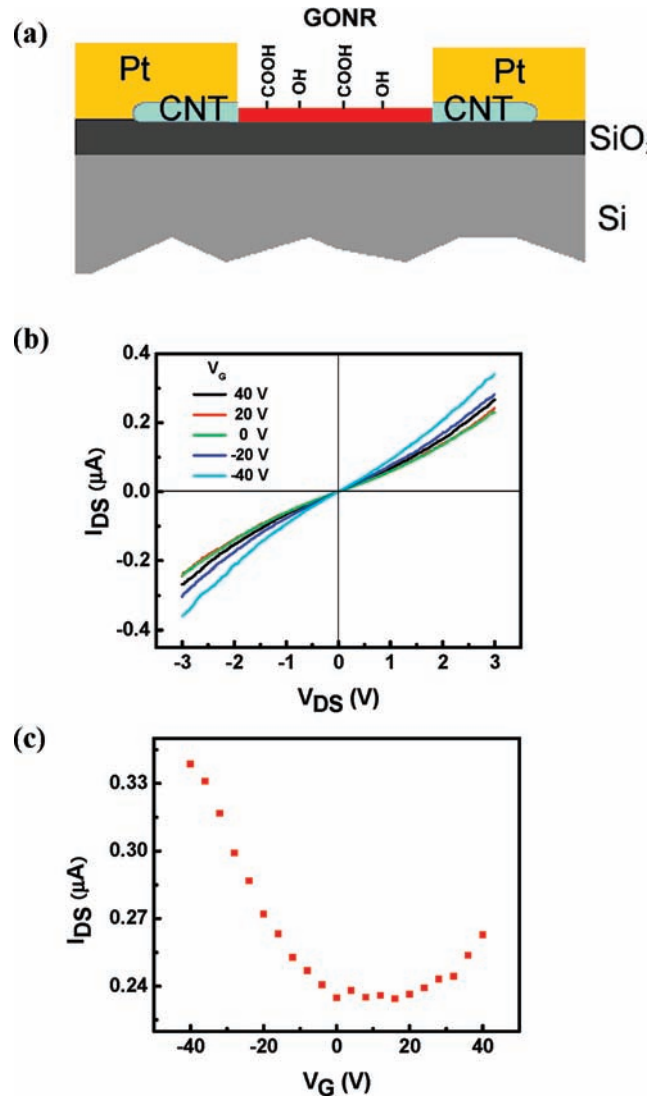

Figure 4. (a) Schematic of the as-unzipped GONR device prior to annealing. (b) $I_{DS}-V_{DS}$ curves of the as-unzipped device at different gate voltages. (c) $I_{DS}-V_G$ data points of the as-unzipped device at a bias voltage of 3 V between source and drain. The electrical characteristics exhibit ambipolar FET behaviors.

MWCNTs under the electrodes in the device are protected from unzipping, so that the contact between the electrodes and the nanostructure should not be changed. Thus, the changes in the electrical properties of the devices are due mainly to modifications of the MWCNTs between the two electrodes. The MWCNT-based device shows excellent metal conductivity before unzipping and good Ohmic contact between the MWCNT and Pt electrodes. At 1 V, the current through the device increases to 200 μA (Figure 3a). The GONR device exhibits relatively poor conductivity, decreasing almost 4 orders of magnitude compared to that before unzipping (Figure 3b). The thermal treatment improves the conductivity of the device (Figure 3c) to about 1 order of magnitude less than that of the MWCNT device in Figure 3a.

The electrical properties of GO nanostructures are much like semiconductors.[25] As shown in Figure 4b, the $I_{DS}-V_{DS}$ behavior of the as-unzipped GONR device shows slight nonlinearity, which is a typical characterization of semiconductor. The field-effect transistor (FET) properties of the as-unzipped GONR devices were further characterized at room temperature under high vacuum (10^{-6} Torr) to minimize adsorption-induced effects

(21) Kim, Y. A.; Hayashi, T.; Endo, M.; Kaburagi, Y.; Tsukada, T.; Shan, J.; Osato, K.; Tsuruoka, S. *Carbon* **2005**, *43*, 2243–2250.
(22) Kudin, K. N.; Ozbas, B.; Schniepp, H. C.; Prud'homme, R. K.; Aksay, I. A.; Car, R. *Nano Lett.* **2008**, *8*, 36–41.
(23) Berciaud, S.; Ryu, S.; Brus, L. E.; Heinz, T. F. *Nano Lett.* **2009**, *9*, 346–352.
(24) Yang, D. X.; Velamakanni, A.; Bozoklu, G.; Park, S.; Stoller, M.; Piner, R. D.; Stankovich, S.; Jung, I.; Field, D. A.; Ventrice, C. A.; Ruoff, R. S. *Carbon* **2009**, *47*, 145–152.

from air exposure;[26] however, since no special precautions, such as high-temperature annealing or long-term evacuation (>6 h), were used to remove trace molecular adsorbates, the shape of the transfer characteristics curve could be affected.[27] Figure 4b shows the $I_{DS}-V_{DS}$ curves recorded at different gate voltages from −40 to 40 V, and Figure 4c shows the $I_{DS}-V_G$ curve at a bias voltage of 3 V between source and drain. The characteristics of the device are similar to the reported ambipolar FETs of metal-CNT contact devices.[28,29] The gradual decrease of the magnitude of the gate voltage in the negative region (from −40 to 0 V) leads to the decrease of the conductivity. This is the typical characteristic of a p-type FET. At the gate voltage of about 0 V, the conductivity declines dramatically. But the high positive gate voltage converts the FET from p-type to n-type.[30]

The yield of the device conversion is high. We fabricated ∼20 MWCNT-based devices with only two of them failing to be converted to GONR devices (data from five devices is shown in the Supporting Information). The semiconducting behavior of the GONRs could be due to the oxygenated[7] species at the edges and the planes; these can act as deep electron traps.[8]

Conclusion

In summary, we have developed a method to convert MWCNT devices into GONRs. Raman spectroscopy was used to monitor the converting process. The as-unzipped GONR devices exhibit electronics characteristic of FETs. The results here demonstrate a simple method to build GNR devices based on MWCNT devices.

Acknowledgment. We thank T. He and A. Higginbotham for their assistance. The MWCNTs were a gift from Mitsui & Co., Ltd. The work was funded by the US Department of Energy's Office of Energy Efficiency and Renewable Energy within the Hydrogen Sorption Center of Excellence (DE-FC-36-05GO15073) and the Air Force Research Laboratory through University Technology Corporation, 09-S568-064-01-C1.

Supporting Information Available: SEM images of five additional devices. This material is available free of charge via the Internet at http://pubs.acs.org.

JA9045923

(25) Wu, X. S.; Sprinkle, M.; Li, X. B.; Ming, F.; Berger, C.; de Heer, W. A. *Phys. Rev. Lett.* **2008**, *101*, 026801.
(26) Kang, D. K.; Park, N.; Hyun, J.; Bae, E.; Ko, J.; Kim, J.; Park, W. *Appl. Phys. Lett.* **2005**, *86*, 093105.
(27) Schedin, F.; Geim, A. K.; Morozov, S. V.; Hill, E. W.; Blake, P.; Katsnelson, M. I.; Novoselov, K. S. *Nat. Mater.* **2007**, *6*, 652.
(28) Martel, R.; Derycke, V.; Lavoie, C.; Appenzeller, J.; Chan, K. K.; Tersoff, J.; Avouris, P. *Phys. Rev. Lett.* **2001**, *87*, 256805.
(29) Zhou, Z.; Eres, G.; Jin, R. Y.; Subedi, A.; Mandrus, D.; Kim, E. H. *Nanotechnology* **2009**, *20*, 085709.
(30) Derycke, V.; Martel, R.; Appenzeller, J.; Avouris, P. *Nano Lett.* **2001**, *1*, 453–456.